Linking soil N dynamics and plant N uptake by means of sensor support

F. Argento [a,b,c,*], F. Liebisch [b,c], M. Simmler [a], C. Ringger [c], M. Hatt [a], A. Walter [b], T. Anken [a]

[a] *Digital Production, Agroscope, Tänikon 1, 8356 Ettenhausen, Switzerland*
[b] *Institute of Agricultural Sciences, ETH Zürich, Universitätstrasse 2, 8092 Zürich, Switzerland*
[c] *Water Protection and Substance Flows, Agroscope, Reckenholzstrasse 191, 8046 Zürich, Switzerland*

ARTICLE INFO

ABSTRACT

Monitoring the spatial and temporal plant availability of nitrogen (N) in agroecosystems is a key step to improve the synchronization between N fertilizer application and crop N demand, consequently reducing the risk of N emissions to the environment. Using a winter wheat N fertilization dataset from six site-years, we linked dynamic nitrate data measured in the soil solution to standard soil and crop analyses data and multispectral imagery acquired by an unmanned aerial vehicle. Wheat N uptake was determined as remotely estimated N uptake (REN) from the spectral data with a power regression model (mean absolute error = 17 kg N ha^{-1}). The nitrate-N in the soil solution (NSS), extracted by means of suction cups, was measured with an ion-selective electrode. The REN proved to be suitable for monitoring the accumulation of N in the plants along the season. The NSS was characterized by low values and found of limited use as a direct indicator for potentially plant-available N. The N balances resulted in N surplus in the range of 43–100 kg N ha^{-1} over the six site-years. The most important contribution to the N balances was the soil N supply (67–143 kg N ha^{-1}; mineralization and atmospheric input). Including this factor in the fertilization strategy was investigated post-season by calculating the 'adjusted N fertilization norm', reflecting the current best fertilization practice in Switzerland. The approach suggested lower N fertilization rates in the fields with higher N surplus. However, such static empirical strategies do not allow to react to in-season changes. Sensor-based monitoring could help to overcome this shortcoming.

Nomenclature

ANFN	Adjusted nitrogen fertilization norm
GDD	Growing degree day(s)
MAE	Mean absolute error
MAPE	Mean absolute percentage error
N_{app}	Nitrogen application
N_{conc}	Nitrogen concentration
N_{up}	Nitrogen uptake
NDRE	Normalized difference red-edge
NF	No fertilizer
NSS	Nitrate-nitrogen in the soil solution
REN	Remotely estimated nitrogen uptake
RMSE	Root-mean-square error
SNS	Soil nitrogen supply
ST	Standard treatment
UAV	Unmanned aerial vehicle
WC	Water content

1. Introduction

Synchronization between nitrogen (N) supply and crop demand is the key to optimizing yield and profit while minimizing environmental impact in both large-scale and medium- to small-scale agricultural systems (Cassman et al., 2002). Modern data-driven technology offers ways to approach such synchronization by supporting real-time monitoring of the processes involved in the N supply and N demand by the plants (Zaks and Kucharik, 2011).

The plant availability of N in agricultural soils is (co-)determined by soil bio-physicochemical factors including soil organic matter content, clay content, soil temperature, soil water content (WC), topography (Tremblay et al., 2011) as well as soil microbial diversity and activity (Jarvis et al., 1996; Murphy et al., 2000). Crop rotation and management are also important determinants (Clivot et al., 2017). When the inputs and in-situ production of plant-available soluble N compounds, primarily nitrate, exceed the plant N uptake, the risk of emissions to the environment is elevated (Sainju, 2017). Excess nitrate readily leaches into ground water, threatening human health (Lassaletta et al., 2014). At

present, combining knowledge of the plant-available N pool in the soil and of the accumulated N in the crops with a good prediction of the total N accumulation by the crop until harvest allows estimating the additional amount of N fertilizer that has to be applied to achieve potential optimal yield (Johnston and Bruulsema, 2014; St. Luce et al., 2011). Besides quantity, the timing of N fertilizer application is important because nitrate and other soluble N compounds are prone to be leached when precipitation exceeds evapotranspiration (Alcoz et al., 1993; Davis et al., 2000). In Central Europe, this happens typically in autumn and winter (Anken et al., 2004; Spiess et al., 2020).

In Swiss winter wheat production, the synchronization between N-supply and plant N demand is commonly approached by dividing the fertilization into three in-season split applications (Chen et al., 2006; Sinaj and Richner, 2017). The recommended timing is based on specific growth stages during tillering (N1), beginning of stem elongation (N2), and ear emergence (N3). The in-season fertilizer distribution is still debated among experts (Levy and Brabant, 2016; Sieling and Kage, 2021) and often farmers define the amount of the splits out of habit and not according to the plant's need as manifested in the field (Ravier et al., 2018). Sinaj and Richner (2017) proposed to adjust the first split by considering the previous crop and the leftover amount of mineral N in the soil in spring (N_{min}, Walther et al., 1994). The in-season adjustments of the second and third split might best be based on the current plant-available N in the soil and the current crop N demand, which could both potentially be estimated with sensor-based methods (Diacono et al., 2013; Samborski et al., 2009). Today, multispectral sensors collecting information in high spatial and/or temporal resolution are widely used in research and precision farming practice. Mounted on tractors (Bean et al., 2018; Bushong et al., 2018; Gnyp et al., 2016), unmanned aerial vehicles (UAV; Aasen et al., 2018; Argento et al., 2020; Chen et al., 2019), or satellites (Jin et al., 2017; Lausch et al., 2019; Yuzugullu et al., 2020), these sensors are used to monitor crop development and nitrogen uptake.

A range of well-established methods can provide information about the dynamics of N availability in soil during the season (Preza Fontes et al., 2019). They are based on continuous soil solution sampling, passive sampling based on ion exchange resins, and incubation experiments (Adamchuk et al., 2004). Some automated sampling systems are on the market, e.g. sampling vehicles and sampling robots, but they are still expensive, labour intensive, and limited to low spatial and temporal resolution. *In-situ* soil nitrate sensors, which would observe the content of available N in the soil in real-time and thus alleviate many drawbacks of the established methods, are not yet fully operational (Rogovska et al., 2019) but topic of recent research (Ali et al., 2019). Independent of the source and applied methodology, dynamic data is key for a decision-making that will allow the land managers to adjust their fertilization strategies to changing weather conditions and actual crop growth during the season. Sensors have the potential to provide this data on the spatial and temporal scales, allowing easy, multi-sourced, and real-time data collection (Chaudhary et al., 2004; Pan et al., 2013). Given that suitable sensors might soon become available, knowhow on their use in decision support is needed.

To advance the knowledge on using dynamic sensor information from soil and plant N for N fertilization decision support the primary objectives of this study were: (i) to develop an indicator for remotely estimated N uptake (REN) by the crop and to investigate how this indicator is linked to nitrate in soil solution (NSS). The secondary objective was: (ii) to calculate the N balance and N use efficiency and discuss it in relation to the sensor-based field management.

2. Materials and methods

2.1. Experimental fields and soil characteristics

The experimental fields were part of a multi-site-year experiment on site-specific N management in winter wheat (*Triticum aestivum* L.)

located on the Swiss Future Farm in Ettenhausen, Switzerland (47.4790021°N, 8.9059287°E). The experimental plots received either uniform application of fertilizer (standard treatment, ST), variable rate application of fertilizer, a control treatment with more fertilizer, or a control treatment without fertilizer. Details about the study design and setup can be found in Argento et al. (2020). In this study, six ST plots corresponding to six site-years were analysed. They were located on six different fields, thus we will henceforth use the field name to identify the site-years. Fields F2, F3, and F4 were used in growing season 2018/2019 and F5, F6, and F7 in 2019/2020 (Fig. 1). These ST plots received a spatially uniform application of 160 kg N ha^{-1} granular ammonium nitrate fertilizer divided into three split applications during the growing season.

The winter wheat cultivar was *Arnold* (Saatzucht Donau, Austria) in 2018/2019 and *Montalbano* (Agroscope/DSP-Delley, Switzerland) in 2019/2020. The fields were managed according to common Swiss practice complying with the ecological performance certificate (ÖLN) needed to receive direct payments from the federal government (state subsidies). Field F4 followed temporal grassland, while the previous crops for the other fields were maize (F2, F3, and F5), sugar beet (F6), and rapeseed (F7), respectively (Table 1). For reducing the influence of mineralization of organic fertilizers, mineral fertilizer was used. However, it is common practice to apply organic fertilizers in Swiss agriculture. Therefore, mixed cattle and pig slurry (35–50 m^3 ha^{-1} in F2–F4) and cattle manure (11 and 7 t ha^{-1} in F5 and F7, respectively) had been applied in the year before the experiment. The field F6 had not received organic fertilizer. Plant protection was kept at the minimum necessary to avoid extended damage that would influence the outcome of the experiment. Mechanical weeding with a 15 m precision tine harrow (Treffler, Germany) and chemical weeding with a combination of contact herbicides (Pacifica Plus and Mero, Bayer, Germany) were performed at the beginning of spring. A growth regulator (CCC 720, Bayer, Germany) was applied in 2020. Fields F4 and F7 were sown later compared to the other site-years (Table 1). On F4, the late sowing in combination with inappropriate weed management negatively affected the growth during the season as reflected by a largely heterogeneous canopy and reduced yield. No negative effects of the late sowing were observed on F7.

Samples of the topsoil (0–20 cm; composite samples of four to six cores) were collected next to the monitoring stations (see section 'soil monitoring') in autumn or in early spring within the two years of the experiment. The samples were analysed for pH, organic carbon content (C_{org} in percentage by weight, wt%) derived from measurements of soil organic matter, and clay content (wt%) as described in Argento et al. (2020). The soil pH was slightly acidic in F2 and F3 and slightly alkaline in the other fields (Table 1). The C_{org} contents ranged from 1.3 wt% for F3 to 3.8 wt% for F7. The clay contents were similar for fields F3–F7 (26–29 wt%), while F2 showed a considerably higher content (40 wt%). The contents of mineral N (N_{min}, 0–90 cm, kg N ha^{-1}) varied between 18 kg N ha^{-1} for F3 and 58 kg N ha^{-1} for F4 (Argento et al., 2020).

2.2. Soil monitoring

On each field, a soil monitoring station was installed on one ST plot to collect soil solution for nitrate analysis and to measure soil temperature and soil volumetric water content (WC, percentage by volume, vol %) with four Drill & Drop soil sensors (Sentek, Stepney, Australia). Each of these four sensors recorded data at six soil depths in the range of 0–60 cm (one measurement point every 10 cm). The calibration for WC, as provided by the manufacturer, assumes a porosity of 50 vol% (Sentek, 2011), which is reasonable for the soils in this study. The sensors reported the WC contents as volume percentage, i.e., the percentage of soil bulk volume being occupied by water. Measurements were recorded at 15 min intervals on a DS3 data logger, which sent the data every 60 min via GSM (Global System for Mobile communication) to the Climaps online database (Sensorscope, Lausanne, Switzerland).
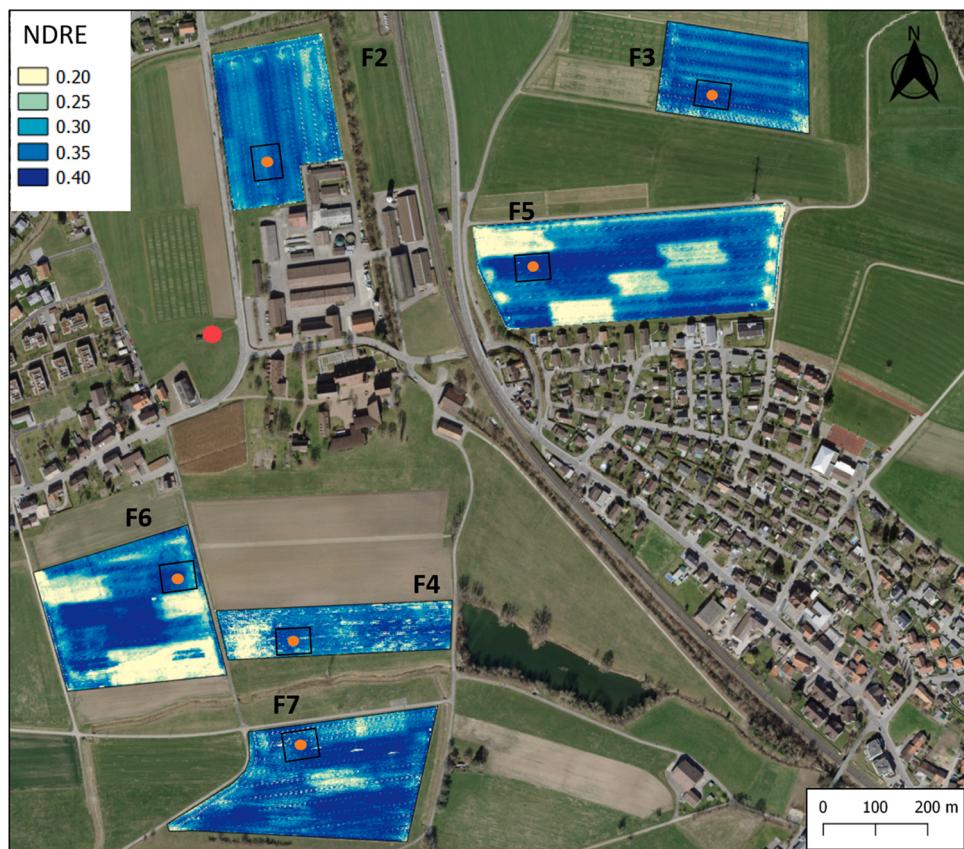
Fig. 1. Map of the experimental fields (F2–F7) with the location of the six soil monitoring stations (small orange dots) and the weather station (large red dot). As an example, the normalized difference red edge (NDRE) index based on multispectral images from mid-May is shown for the different wheat fields in 2019 (F2, F3, and F4) and in 2020 (F5, F6, and F7). (For interpretation of the references to colour in this figure legend, the reader is referred to the web version of this article.)

Soil pore water, referred to as 'soil solution', was collected by a solar-powered semi-automatic sampling system with a vacuum pump connected to eight suction cups, placed in the soil at two depths (four at 15 cm and four at 45 cm). Each suction cup was composed of a hollow metal tube connected to a porous ceramic cup (round bottom, tapered neck, 1 bar high flow, Soilmoisture Equipment Corp., Santa Barbara, CA, USA). To facilitate the soil solution extraction and collection in the hollow tube, a vacuum of − 600 mbar was maintained by the pump that was automatically operated on demand upon sensing pressure changes. Once per week, the solution collected over a period of 48 h was pumped into a graduated bottle, transferred to the laboratory, and immediately analysed. The solution was passed through a 0.2 μm regenerated cellulose syringe filter (Lab Logistics Group, Meckenheim, Germany) and mixed 1:1 with an interference suppressor solution (Mettler-Toledo, Columbus, OH, USA) to adjust ionic strength and reduce interference from other ions. The electrochemical potential in mV was measured with an ion-selective electrode (perfectION comb NO_3, Mettler-Toledo, Columbus, OH, USA) and converted to nitrate concentrations with a three-point calibration (10–100 mg L^{-1}) based on dilutions of a standard solution (ISE standard NO_3 1000 mg L^{-1}, Mettler-Toledo, Columbus, OH, USA) mixed 1:1 with interference suppressor solution. For both topsoil (0–30 cm, corresponding to suction cup at 15 cm) and subsoil (30–60 cm, suction cup at 45 cm), the nitrate-N in the soil solution (NSS, kg N ha^{-1}) was calculated from the nitrate concentration (kg NO_3 L^{-1}), the WC (vol% = L dm^{-1} m^{-2}), and the height of the soil layer (H, dm) according to Eq. 1 (0.226 is the molar conversion factor). The corresponding values for topsoil and subsoil were then summed to obtain the total NSS per unit area over a 60 cm thick soil layer.

$$NSS = (NO_3 * 0.226) * WC * H * 10^4 \quad m^2 ha^{-1} \qquad (1)$$

2.3. Environmental monitoring

The local climate data including daily minimum and maximum air temperature (°C) and daily precipitation (mm) were collected from a weather station (WIGOS-ID 0–20000–0–06679) located in proximity of the fields (Fig. 1) and operated by the Swiss Federal Office for Meteorology (MeteoSwiss). Daily temperature was aggregated to phenologically meaningful growing degree days (GDD) according to Eq. 2.

$$GDD = \frac{Tmax + \max(Tmin, \ Tbase)}{2} - Tbase \qquad (2)$$

Table 1
Selected topsoil (0–20 cm) properties, namely pH, organic carbon (C_{org}, percentage by weight, wt%), clay content (wt%), and mineral nitrogen content (N_{min}, 0–90 cm, kg N ha^{-1}) collected over the six experimental site-years (fields F2–F7) in the proximity of the soil monitoring stations. Also listed are the date of wheat sowing and the type of previous crop.

Field	Sowing date	Previous crop	pH[a]	C_{org}[b] wt%	Clay[c] wt%	N_{min}[d] kg N ha^{-1}
F2	2018–10–09	Maize	6.6	2.3	40	34
F3	2018–10–12	Maize	6.8	1.3	26	18
F4	2018–11–05	Temporal grassland	7.6	3.2	29	58
F5	2019–10–24	Maize	7.7	1.6	27	31
F6	2019–10–26	Sugar beet	7.8	1.9	28	43
F7	2019–11–14	Rapeseed	7.7	3.8	27	37

[a] H_2O method (solid:solution ratio 1:5)
[b] C_{org} = organic carbon = soil organic matter/1.724 (Howard, 1965)
[c] Soil particles < 2 μm
[d] Beginning of spring growth (Feb)

Where T_{max} and T_{min} are the daily maximum and minimum temperatures, respectively, and T_{base} is the so-called base temperature, which was set to 0 °C (Grieder et al., 2015). The cumulative sums of GDD and precipitation over the growing season are shown in Fig. 2.

2.4. Monitoring plant nitrogen uptake

During the growing season, the fields were monitored weekly by means of a UAV (Phantom 4 Pro, DJI, China) equipped with a Parrot Sequoia sensor system (Parrot, France), which includes a multispectral camera and a radiation sensor for radiometric correction. Radiometrically calibrated spectral reflectance maps were obtained for the spectral bands green (550 ± 40 nm), red (660 ± 40 nm), red-edge (RE, 735 ± 10 nm), and near infrared (NIR, 790 ± 40 nm). Details on flight conditions, radiometric calibration, and raw data handling can be found in Argento et al. (2020). We developed an empirical model to estimate the total N uptake in the above-ground crop biomass (kg N ha^{-1}) from multispectral data. We refer to these estimates as remotely estimated N uptake (REN, kg N ha^{-1}). Ground truth data for N uptake (N_{up} = biomass per area * N_{conc} in crop) was collected at specific growth stages (BBCH 23, 31, and 37 according to Meier et al., 2009) on the day of the corresponding UAV flight from an undisturbed 5 m^2 area of crop in proximity of the soil monitoring stations. In total, the dataset consisted of 295 samples of ground truth crop N uptake and corresponding multispectral data from multiple plots in the six site-years. The programming language R version 3.6.3 (R Core Team, 2020) was employed for model training and validation. Power regression with the spectral index Normalized Difference Red-Edge [NDRE = (NIR − RE) / (NIR + RE); Barnes et al. (2000)] as predictor variable was conducted with the base R function *nls*. Model performance was determined on the training set and in leave-one-field-out cross-validation, i.e. using data of five of six fields for training and validating the model on the left-out field. Additionally, REN was compared to ground truth N_{up} using Passing-Bablok regression with the R package *mcr* (Manuilova and Schuetzenmeister, 2021) and Lin's concordance correlation analysis with the R package *DescTools* (Signorell, 2021).

2.5. Nitrogen balance

The N balance was calculated from soil N supply (SNS, kg N ha^{-1}), N input from fertilizer (N_{app}, kg N ha^{-1}), and N uptake by the plants (N_{up},

kg N ha^{-1}) according to Eq. 3. The SNS was estimated as the N uptake by the plants observed for the full growing season in the no fertilizer controls of the corresponding site-years (Argento et al., 2020; Kindred et al., 2015). This measure for plant-available N provided from the soil system also includes N from atmospheric deposition. The SNS plus the N_{app} is an estimate for the total plant-available N supply over the season. The N balance (kg N ha^{-1}) finally calculates as the difference between total plant-available N and the total N uptake (N_{up}) by the crop (Eq. 3). A positive N balance represents N surplus (kg N ha^{-1}) in the system at the end of the season.

$$N\ balance = (SNS + N_{app}) − N_{up} \qquad (3)$$

The total yield (t ha^{-1}, straw + grain) and the apparent fertilizer recovery [AFR = (N_{up} − SNS)/N_{app}] were used as indicators of the agronomic performance. Moreover, to evaluate the obtained results with respect to the current best N fertilization practice in Switzerland, we calculated the adjusted N fertilizer norm (ANFN) according to the *Principles of Agricultural Crop Fertilization in Switzerland* (Sinaj and Richner, 2017). This method provides fertilizer recommendations that consider several additive correction factors (Eq. 4). In our case, the ANFN value (kg N ha^{-1}), which is based on a crop N removal reference value (norm, kg N ha^{-1}), was adjusted to the location-specific yield expectation (f_{yield}). Furthermore, it was corrected for N release from mineralization of soil organic matter (f_{SOM}), for the tillage ($f_{tillage}$), for residual N of the previous crop in the rotation (f_{PC}), and for N release from organic fertilizer from the previous year ($f_{orgfert}$). Additionally, adjustments according to the winter and spring precipitation ($f_{winterP}$ and $f_{springP}$) were considered.

$$ANFN = norm + f_{yield} + f_{SOM} + f_{tillage} + f_{PC} + f_{orgfert} + f_{winterP} + f_{springP} \qquad (4)$$

3. Results

3.1. Remotely estimated nitrogen uptake

We employed non-linear regression to relate the N uptake by the plants (N_{up}), measured at different stages, to the NDRE calculated from multispectral images (power function, Fig. 3a). The established empirical relationship was used to estimate the N_{up} based on NDRE (remotely estimated N uptake, REN, kg N ha^{-1}, Fig. 3b,).

The model had a mean absolute error (MAE) of 17.2 kg N ha^{-1} and a root-mean-square error (RMSE) of 25.3 kg N ha^{-1} when trained and validated on the full dataset ($n = 295$). Lin's concordance correlation coefficient (CCC) and the Pearson's correlation coefficient (r) between measured N uptake and fitted REN were 0.912 and 0.918, respectively (Fig. 3b). Additionally, the model was validated in leave-one-field-out cross-validation (Table 2). Except for field F2, the model performance in cross-validation was similar to the performance of the full model (MAE ≤ 20% higher in CV than of the full model). For field F2, in which the highest NDRE and N uptake values were observed (Fig. 3a), the performance was substantially lower in cross-validation as compared to the full model (MAE 129% higher in CV than of the full model).

3.2. Dynamics of weather conditions, plant nitrogen uptake, and nitrate-nitrogen in the soil solution

In 2019, the season was characterized by a cumulative precipitation of 295 mm in the most critical period for winter wheat growth in Central Europe from April to June. Soil volumetric WC was 20–50 vol% (Fig. 4e). The temporal distribution of precipitation was even, without prolonged drought periods (Fig. 2b). In 2020, the cumulative precipitation in April to June was 255 mm and thus lower than in the previous year. Furthermore, precipitation was less evenly distributed with prolonged drought periods, notably 32 days without precipitation from end
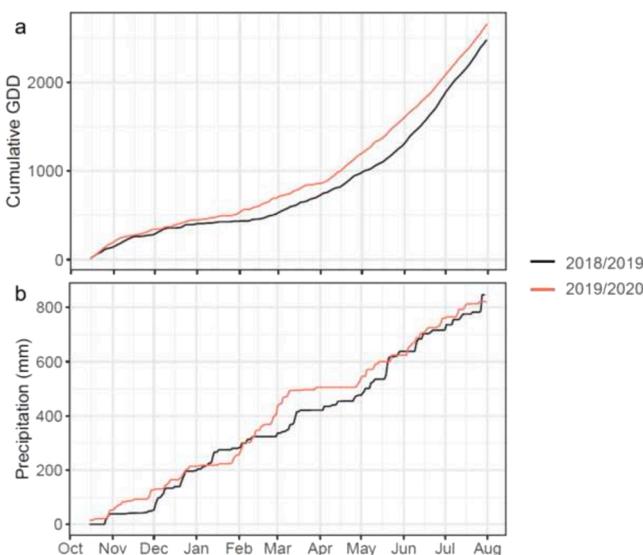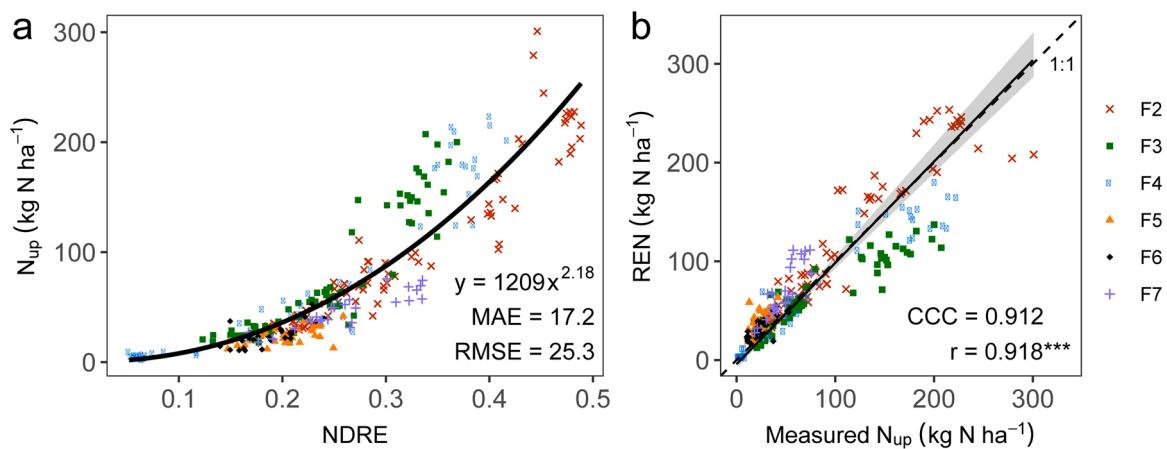

Fig. 2. Cumulative sums of (a) growing degree days (GDD) and (b) precipitation (mm) in 2018/2019 and 2019/2020 over the full winter wheat growing season (Oct–Aug).

Fig. 3. (a) Power regression of nitrogen uptake (N_{up}, kg N ha^{-1}) on Normalized Difference Red-Edge (NDRE) for the six site-years F2–F7 ($n = 295$). MAE = mean absolute error; RMSE = root-mean-square error. (b) Passing-Bablok regression between the measured nitrogen uptake (N_{up}, kg N ha^{-1}) and the remotely estimated nitrogen uptake (REN, kg N ha^{-1}) for the six site-years F2–F7 ($n = 295$, bootstrap 95% confidence band in grey). REN values correspond to fitted values in panel a. The Lin's concordance correlation coefficient (CCC) and the Pearson's correlation coefficient (r) are reported.

of March to end of April (Fig. 2b). Correspondingly, the WC in 2020 was lower than in 2019, ranging from 5 to 25 vol% with a clear depression corresponding to the period of low precipitation (Fig. 4f). The soil temperature (T_{soil}) varied during the season between 5 and 20 °C both in 2019 (Fig. 4g) and in 2020 (Fig. 4h). The cumulative GDD in both winter wheat seasons (Oct–Aug 2018/2019 and 2019/2020) reached values around 2500 (Fig. 2a) with a strong increase in the summer months. Overall, 2020 was warmer than 2019, which was reflected in higher cumulative GDD starting from late winter. Total precipitation (Oct–Aug) was similar between the two growing seasons (Fig. 2b). However, the distribution was less even in 2020 with precipitation peaks, such as in the period Feb–Mar, and, as mentioned above, long periods lacking precipitation in spring.

The values of REN ranged from 5 to 170 kg N ha^{-1} and were similar in 2019 and 2020, although two different wheat varieties were used (Fig. 4a, b). They closely followed the observed N uptake (bars, Fig. 4a, b) until mid-May but increasingly deviated from the observed N uptake values in the late season. In 2019, the development of N uptake was, as expected, almost continuously increasing until mid-May but showed a depression on the fields F2 and F3 in late May and June. This depression is difficult to explain. Since there was no evidence of methodological artefacts, we speculate that it may be a consequence of ear emergence. Comparing 2020 with F2 and F3 from 2019, REN increased at a lower rate in the first but at a higher rate in the second half of the season. This resulted in similar REN levels at the end of the seasons. This pattern is

Table 2
Results of the leave-one-field-out cross-validation of the power regression of nitrogen uptake on the spectral index Normalized Difference Red-Edge (NDRE). The corresponding performance of the full regression model (trained on all fields' data; $n = 295$) is listed for comparison.

	Full model			Leave-one-field-out cross-validation		
	MAPE[a]	MAE[b]	RMSE[c]	MAPE[a]	MAE[b]	RMSE[c]
Field	%	kg N ha^{-1}	kg N ha^{-1}	%	kg N ha^{-1}	kg N ha^{-1}
F2	20	17	25	32	39	61
F3	24	20	31	28	24	35
F4	30	16	25	31	17	28
F5	71	15	18	80	17	19
F6	50	10	11	53	10	12
F7	47	22	27	52	25	29
F2–F7	38.4	17.2	25.3	–	–	–

[a] Mean absolute percentage error
[b] Mean absolute error
[c] Root-mean-square error

related to the 32 days without significant precipitation during the phase of strong growth of winter wheat in March and April, which resulted in delayed crop development and correspondingly delayed N uptake in 2020. The lower N uptake in F4 compared with F2 and F3 (all 2019) was due to late sowing in combination with inappropriate weed management as described in the methods section.

Values of NSS were in a similar order of magnitude in both years and across all fields being between 5 and 15 kg N ha^{-1} at the beginning of the season and generally decreased towards the end of season, reaching values of about 2 kg N ha^{-1} at harvest in 2019 and even lower in 2020 (Fig. 4c, d). One to two weeks after the fertilization events, the NSS was temporally increased in 2019 while in 2020 this was only observed for one of three soils. Across the six site-years, lower NSS values were generally related to higher REN (Fig. 5). However, the temporal development of in-season changes in NSS are poorly reflected in REN. For example, the temporal courses of NSS along the season in 2019 tightly paralleled each other across the three fields, thus not reflecting the strong distinction observed in the temporal development of REN (field F4 versus F5 and F6).

3.3. Nitrogen balance

The N balance was calculated as the sum of SNS and N fertilizer input minus the total N uptake by the plants (Table 3). Same amount of fertilizer was applied for all site-years according to the standard practice in the region (153–155 kg N ha^{-1}). Similar SNS in the range of 123–143 kg N ha^{-1} were observed for the site-years in 2019 and for F7 in 2020. The other two fields in 2020 showed considerably lower SNS, namely 67 and 75 kg N ha^{-1} for F5 and F6, respectively. Total N uptake by the plants was in the range of 165–221 kg N ha^{-1}. Except for F4, higher total N uptake was generally related to higher biomass expressed by the sum of straw and grain yield (Table 3). F4 showed the lowest yield but a comparably high N uptake. The estimated N balance indicated surplus of 43–100 kg N ha^{-1}, with consistently higher values in 2019 (76–100 kg N ha^{-1}) than in 2020 (43–65 kg N ha^{-1}). The apparent fertilizer recovery (AFR) ranged from 35% to 78%, with higher values in 2020 (58–78%) compared with 2019 (35–51%).

We related the common standard practice to the ANFN, which recommended N fertilizer needs (64–145 kg N ha^{-1}) lower than the applied amounts for all fields. A clear trend of reduced N fertilizer recommendation with increased N surplus was apparent (Table 3). The largest correction factor for the adjusted fertilizer recommendation was the applied organic fertilizer in the previous year ($f_{orgfert}$), which was particularly high in F4, for which the lowest fertilizer amounts were
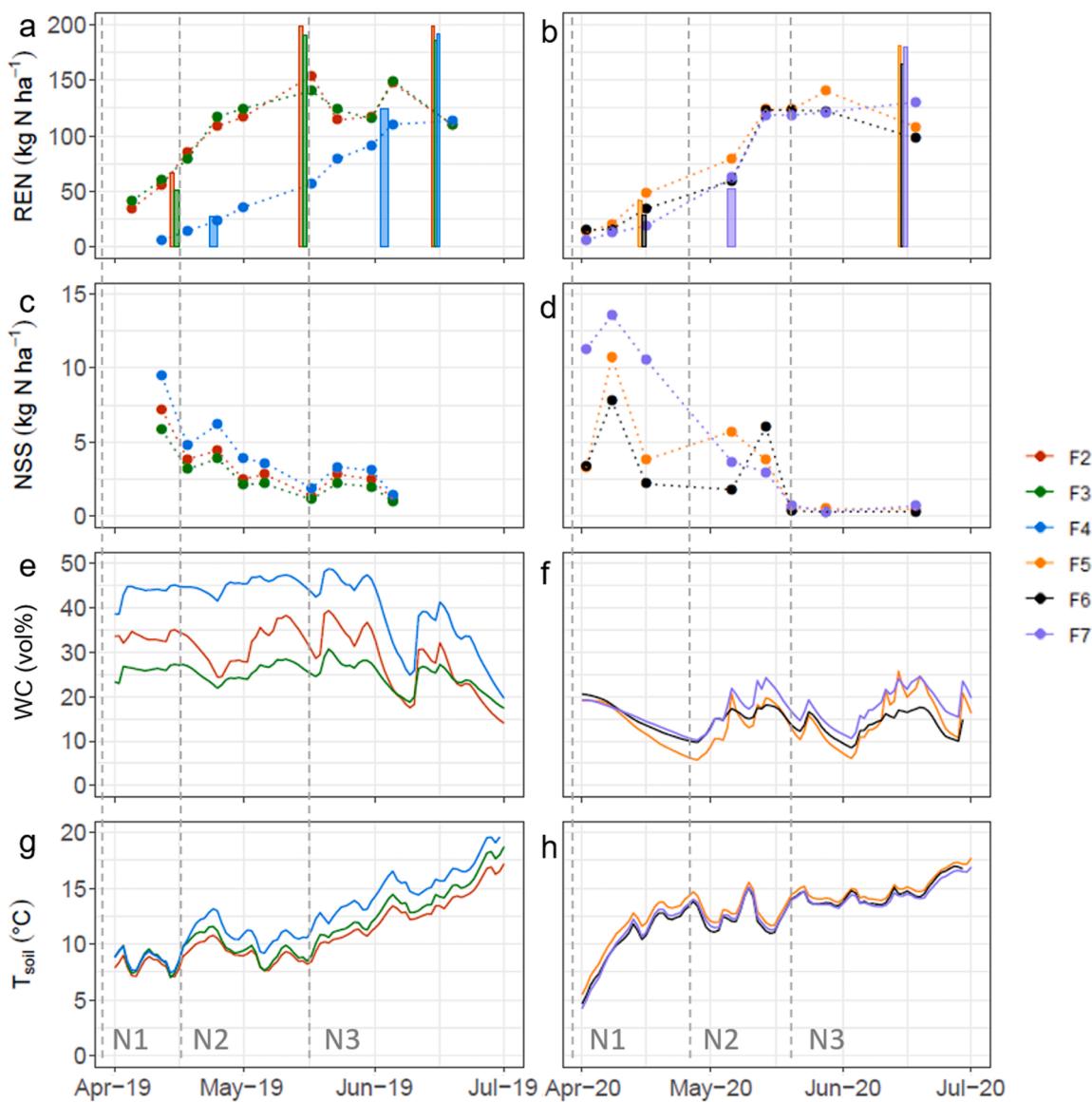
Fig. 4. Dynamic agronomic and environmental data collected from six site-years: F2, F3, and F4 in 2019 (left panels) and F5, F6, and F7 in 2020 (right panels) for a period of three months each (Apr–Jun). From top to bottom, the panels show (a, b) the remotely estimated N uptake (REN, kg N ha^{-1}) by the crop with the nitrogen uptake measured in the biomass (dashed bars), (c, d) the nitrate-N in the soil solution (NSS, kg N ha^{-1}), (e, f) the volumetric water content (WC, vol%) of the soil, and (g, h) the soil temperature (T_{soil}, °C). WC and T_{soil} represent averages across the 6 measurements from 0 to 60 cm soil depth. The vertical dashed lines indicate the time-points of the three split fertilizations (N1, N2, and N3).

recommended (Table 3; correction factors in Supplementary Table S1 and Supplementary Fig. S1).

4. Discussion

4.1. Dynamic indicators for crop N and potentially plant-available N

In this study, we aimed to advance the knowledge on using dynamic sensor information from soil and plant N for N fertilization decision support. Using a six site-year winter wheat experiment dataset, we investigated remotely estimated N uptake (REN) as indicator for N in crops and nitrate-N in the soil solution (NSS) as a real-time indicator for the potentially plant-available N in soil. The relationship between N uptake by the plants and the multispectral NDRE (Fig. 3) showed that multispectral imagery is able to monitor N uptake as reported in previous studies (Homolová et al., 2013; Li et al., 2014). The approach shown here using drone-based data is also applicable to satellite-derived

data (Scharf et al., 2002; Wang et al., 2017). In this case, larger areas can be monitored, but the lower spatial resolution results in a loss of spatial precision (Crema et al., 2020). A robust calibration for N uptake being valid for the full vegetative growth phase is needed when the data is aimed for decision support for fertilization. In our case, residuals of the calibration model tended to increase at higher N in crops, corresponding to later growth stages in the late phase of the season (Fig. 3), when fertilization is typically finished. The increased uncertainty at high plant N is largely related to saturation of the spectral index, which goes along with slowly loosing sensitivity as indicated by the curvature of the calibration curve. Additionally, the spectral response of the wheat plants changes with the crops transition to generative growth characterized by spike pushing, which reduces the sensitivity of the spectral index for N uptake (Argento et al., 2020; Kancheva and Georgiev, 2013). In leave-one-field-out cross-validation, we observed that the model is robust with respect to the different site-years. Only for field F2 the performance in cross-validation substantially differed from the
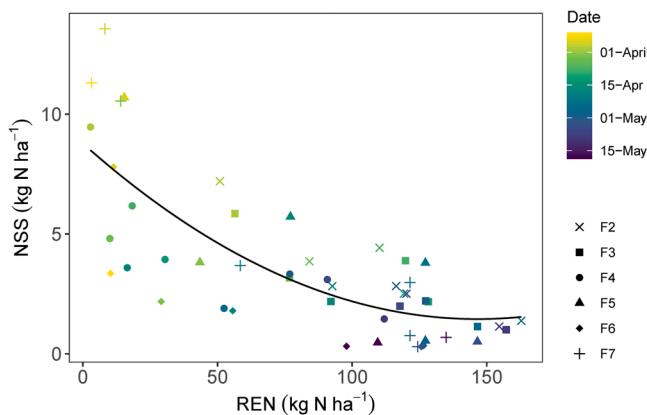
Fig. 5. Relationship between nitrate-nitrogen in the soil solution (NSS, kg N ha^{-1}) and remotely estimated nitrogen uptake (REN, kg N ha^{-1}) by the crop for the six site-years (F2–F7, shapes). The black trend-line is shown as an eye-guide to the relationship. The colour represents the time of monitoring of the respective REN and NSS (April to mid-May).

performance of the full model (trained on all data, Table 2). In this field, the highest REN and NDRE values were observed (Fig. 3). This indicates that extrapolation beyond the growth conditions covered in the calibration dataset might significantly deteriorate the performance of the calibration. From other studies it is known, that the cultivar can have an effect on the reflectance characteristics (Pinter et. al, 1985). However, in our study we did not see indication for substantial differences in the NDRE to N relationship that we attributed to the two different cultivars we used.

Nitrate-N in the soil solution (NSS) extracted by suction cups was evaluated as a means to inform on supply or depletion of plant-available nitrogen in the soil during the season. This, in anticipation of in-situ soil solution nitrate sensors like the one by Ali et al. (2019) being available in the future. The NSS values in our study decreased from already low levels in April (6–14 kg N ha^{-1}) to very low levels at harvest of 1–4 kg N ha^{-1} (Fig. 4). We expected this decrease as the uptake of available nitrate by the growing crop (Fig. 4c, d) and unknown losses presumably exceed the replenishment of the nitrate pool in the soil through fertilization, mineralization, and other sources. Comparing the size of the NSS pool in the order of 1–10 kg N ha^{-1} to the uptake rates of the plants of on average around 15 kg N ha^{-1} per week in April and May, it becomes apparent that the NSS pool is small compared to the N pool that became plant available during the season. In typical agricultural soils, the highly soluble and readily plant available NO_3^- is typically by far the most predominant plant-available inorganic N compound in soil solution (Kabala et al., 2017), even when receiving NH_4^+-containing fertilizers (Quan et al., 2016). Ammonium (NH_4^+) can be taken up by plant roots to serve the plants N demand. However, most NH_4^+ in agricultural soils is rapidly converted to nitrate (NO_3^-) by microbial oxidation in the process of nitrification (Norton and Ouyang, 2019; Inselsbacher et al., 2013). As nitrate is the dominant N form taken up by the plants in agricultural soils, we thus conclude that the small NSS pools in our study were characterized by steady influxes, approximately balancing the plant uptake. N mineralization followed by rapid nitrification and dissolution of applied mineral fertilizer release nitrate to the soil solution. Atmospheric deposition additionally contributes. Most of the nitrate released to the soil solution may be immediately assimilated by microbial biomass and plant roots, resulting in comparably low net concentration in soil solution (Ottow, 2011). Accordingly, 1–2 weeks after fertilizer applications of 25–70 kg N ha^{-1} we observed only small to negligible increases in NSS of around 0–2 kg N ha^{-1} as compared to the levels shortly before the fertilizer application (Fig. 4). After the third fertilizer split application of 25 kg N ha^{-1} in June, the REN and the corresponding ground truth data indicated no substantial further plant

uptake of N in both years (Fig. 4). Also, NSS did only increase by less than 1.5 kg Nha^{-1} in 2019 and not increase at all in 2020. Therefore, rapid and extensive incorporation into microbial biomass is suspected, as leaching can be ruled out due to the absence of strong rain events.

Lower NSS values tended to occur later in the season at higher REN values (Fig. 5), reflecting the link to plant uptake. However, within season variation in NSS did poorly mirror changes in REN, which correspond to the extraction of plant-available N from the soil. Therefore, NSS appears to be of limited use as a direct indicator of potentially plant-available N in soils. In our case, the comparably small NSS net concentrations were governed by comparably large fluxes with kinetics known to be highly influenced by environmental conditions — e.g., mineralization and N assimilation by microbial biomass and roots are highly sensitive to soil temperature and moisture. The fields from 2019 nicely illustrate the poor performance of NSS as a direct indicator of plant available N. Because of inappropriate management, the N uptake in F4 was much lower than in F2 and F3 in spring, but compensated later in the season (Fig. 4). Accordingly, the NSS values in F4 versus F2 and F3 were slightly higher in the early season. However, NSS developed very similar over the season in the three fields and failed to indicate the different dynamics of the extraction of plant-available N.

4.2. Nitrogen balance

The achieved grain yields of about 6–7 t ha^{-1} (Argento et al., 2020) and N uptakes of 165–221 kg ha^{-1} represent typical values for Switzerland (Sinaj and Richner, 2017) and the region (Maltas et al., 2015). Although total N uptake did not differ considerably between fields and years, the N surplus calculated from the N balance (Table 3) was higher in 2019 (76–100 kg N ha^{-1}) compared to 2020 (43–65 kg N ha^{-1}). The difference is attributable to higher soil N supply (SNS) of 127–143 kg N ha^{-1} in 2019 versus 67–123 kg N ha^{-1} in 2020. These values are in the range of values reported in the literature for winter wheat cropping systems: Kindred et al. (2015) found that SNS varied spatially, with values of 120, 75, and 60 kg N ha^{-1} in three different site-years. Hartmann et al. (2014) showed an apparent net mineralization of 64 and 84 kg N ha^{-1}. St. Luce et al. (2011) and Stevens et al. (2005) confirmed the importance of soil N mineralization and reported values in the range of 50–80% of the total N uptake by the plants, which is in line with our results. The apparent fertilizer recoveries of 35–78% on the studied fields compare well with values observed by Hausherr

Table 3

Nitrogen (N) balance for six site-years of winter wheat cropping systems. All contributions to the N balance, namely the soil N supply (SNS), the N fertilizer application (N_{app}), and the total N uptake (N_{up}), are expressed in kg N ha^{-1}. Additionally, the agronomic performance in terms of total yield (t ha^{-1}) and apparent fertilizer recovery (AFR, %) is given.

Field	F2	F3	F4	F5	F6	F7
N balance (kg N ha^{-1})						
Total supply of plant available N	297	280	292	222	230	278
Soil N supply (SNS)[a]	143	127	138	67	75	123
N fertilizer application (N_{app})	154	153	154	155	155	155
Total N uptake (N_{up})	221	185	191	178	165	219
N surplus	76	95	100	43	65	59
Agronomic performance						
Total yield[b] (t ha^{-1})	18.1	16.5	13.9	15.1	14.9	18.4
AFR[c] (%)	51	37	35	78	58	62
Best fertilization practice						
ANFN[d] (kg N ha^{-1})	124	109	64	123	130	145

[a] Supply from soil and atmospheric deposition (determined from the N uptake on the control plots with no fertilizer)

[b] Total yield = grain yield + straw yield

[c] Apparent fertilizer recovery

[d] Adjusted N fertilization norm

Lüder et al. (2020) and Hategekimana et al. (2012).

The above findings highlight the high importance of including soil N supply in the fertilization strategy in order to reduce N surpluses. One approach is implemented in the 'adjusted N fertilization norm' (ANFN). This static empirical method allows a more efficient fertilization and a reduction of N surplus compared to the common standard practice (Maltas et al., 2015). However, it is based on tabulated reference values and takes neither dynamic data (e.g. 3 months average of precipitation) nor data representing in-field variability into account. In the future, these shortcomings might be overcome with advanced models using in-season sensor-based and weather data from single or multiple sources. A recent simulation study by Pedersen et al. (2021) found a combined use of crop sensor and soil information beneficial to improve N use efficiency. Models based on dynamic data should also include an estimation of N release from soil and a prediction of potential yield and need to be well calibrated to be reliably applied for fertilization decision support (Yin et al., 2020). As shown in this study, it is still challenging to gain sufficient information from soil sensors to infer the potential fluxes of N from soil to crop, to be able to improve the in-season N balance.

Given the small size of the dataset of this and similar studies, the generalizability of observed relationships between sensor data and crop response is limited. We therefore advocate for large spatial networks of soil and weather sensors combined with high-resolution monitoring of N uptake via spectral data. Data from such a network may help to clarify whether N supply from soil during the season can be modelled based on sensor information and used for improving fertilization strategies. However, such an approach requires robust and less work-intensive type of sensing devices. A new generation of sensors for soil solution nitrate is currently being developed but yet to be broadly validated under real farm conditions (e.g. BGU, 2020; Fraunhofer, 2020; Teralytic, 2020; Terraquat, 2021). But, as shown in this study, soil solution nitrate data alone seems not informative enough towards the potentially bioavailable N. However, its potential in combination with other data sources in multivariate models has not been explored yet.

5. Conclusion

We investigated a remote sensing-based indicator for crop N uptake and a real time indicator for potentially plant-available N in soil. The indicator 'remotely estimated N uptake' (REN) based on UAV-acquired multispectral images allowed high spatial and temporal resolution monitoring of crop N uptake. The nitrate-N in the soil solution (NSS), monitored on a weekly basis with suction cups, was in general at low levels as compared to the fluxes indicated by the plant N uptake. The lowest NSS values were observed at the end of the season in all studied fields. The dynamics of the extraction of plant-available N from the soil was however poorly represented by NSS. We therefore conclude that weekly measured NSS is of limited use as a direct indicator for potentially plant-available N and for fertilisation management.

The N balances indicated higher N surpluses in 2019 compared to 2020. The higher surpluses could be attributed to higher soil N supply. Including this factor in the fertilization strategy was investigated post-season by calculating the 'adjusted N fertilization norm', the current best practice in Switzerland. This approach suggested lower N fertilization rates in the fields when higher N surpluses were observed. However, such static empirical methods do not facilitate in-season adjustments. Sensor-based monitoring could help to overcome this shortcoming but advances of knowledge on derivation and use of dynamic sensor information from soil and plant N for N fertilization decision support are required.

CRediT authorship contribution statement

Francesco Argento: Conceptualization, Methodology, Formal analysis, Investigation, Data curation, Visualization, Writing – original draft. **Frank Liebisch**: Conceptualization, Writing – original draft,

Supervision, Project administration, Funding acquisition. **Michael Simmler**: Methodology, Data curation, Visualization, Writing – review & editing. **Cecil Ringger**: Data curation, Visualization. **Matthias Hatt**: Investigation. **Achim Walter**: Supervision, Writing – review & editing, Project administration, Funding acquisition. **Thomas Anken**: Conceptualization, Writing – original draft, Supervision, Project administration, Funding acquisition.

Declaration of Competing Interest

The authors declare that they have no known competing financial interests or personal relationships that could have appeared to influence the work reported in this paper.

Data availability

The research data that support the findings of this study are available in the online data repository with the identifier DOI: https://doi.org/10.3929/ethz-b-000516820 at http://hdl.handle.net/20.500.11850/516820 last accessed [25/11/2021].

Appendix A. Supporting information

Supplementary data associated with this article can be found in the online version at doi:10.1016/j.eja.2022.126462.

References

Aasen, H., Honkavaara, E., Lucieer, A., Zarco-Tejada, P.J., 2018. Quantitative remote sensing at ultra-high resolution with UAV spectroscopy: a review of sensor technology, measurement procedures, and data correctionworkflows. Remote Sens. 10, 1–42. https://doi.org/10.3390/rs10071091.

Adamchuk, V.I., Hummel, J.W., Morgan, M.T., Upadhyaya, S.K., 2004. On-the-go soil sensors for precision agriculture. Comput. Electron. Agric. 44, 71–91. https://doi.org/10.1016/j.compag.2004.03.002.

Alcoz, M.M., Hons, F.M., Haby, V.A., 1993. Nitrogen fertilization timing effect on wheat production, nitrogen uptake efficiency, and residual soil nitrogen. Agron. J. 85, 1198–1203. https://doi.org/10.2134/agronj1993.00021962008500060020x.

Ali, M.A., Wang, X., Chen, Y., Jiao, Y., Mahal, N.K., Moru, S., Castellano, M.J., Schnable, J.C., Schnable, P.S., Dong, L., 2019. Continuous monitoring of soil nitrate using a miniature sensor with poly (3-octyl-thiophene) and molybdenum disulfide nanocomposite. ACS Appl. Mater. Interfaces 11 (32), 29195–29206. https://doi.org/10.1021/acsami.9b07120.

Anken, T., Weisskopf, P., Zihlmann, U., Forrer, H., Jansa, J., Perhacova, K., 2004. Long-term tillage system effects under moist cool conditions in Switzerland. Soil Tillage Res. 78, 171–183. https://doi.org/10.1016/j.still.2004.02.005.

Argento, F., Anken, T., Abt, F., Vogelsanger, E., Walter, A., Liebisch, F., 2020. Site-specific nitrogen management in winter wheat supported by low-altitude remote sensing and soil data. Precis. Agric. https://doi.org/10.1007/s11119-020-09733-3.

Barnes, E.M., Clarke, T.R., Richards, S.E., Colaizzi, P.D., Haberland, J., Kostrzewski, M., et al., 2000. Coincident detection of crop water stress, nitrogen status and canopy density using ground based multispectral data. In Proceedings of the Fifth International Conference on Precision Agriculture, Bloomington, MN, USA (Vol. 1619).

Bean, G.M., Kitchen, N.R., Camberato, J.J., Ferguson, R.B., Fernandez, F.G., Franzen, D. W., Laboski, C.A.M., Nafziger, E.D., Sawyer, J.E., Scharf, P.C., Schepers, J., Shanahan, J.S. 2018. Active-optical reflectance sensing corn algorithms evaluated over the United States midwest corn belt. Agron. J. 110, 2552–2565. https://doi.org/10.2134/agronj2018.03.0217.

BGU, 2020. Sensor for Real-time Measurement of Soil Nitrate. ⟨https://in.bgu.ac.il/en/pages/news/sensor_nitrate.aspx⟩ last accessed [11/02/2021 at 15:12].

Bushong, J.T., Mullock, J.L., Arnall, D.B., Raun, W.R., 2018. Effect of nitrogen fertilizer source on corn (Zea mays L.) optical sensor response index values in a rain-fed environment. J. Plant Nutr. 41, 1172–1183. https://doi.org/10.1080/01904167.2018.1434202.

Cassman, K.G., Dobermann, A., Walters, D.T., 2002. Agroecosystems, nitrogen-use efficiency, and nitrogen management. Ambio 31, 132–140. https://doi.org/10.1579/0044-7447-31.2.132.

Chaudhary, S., Sorathia, V., Laliwala, Z., 2004. Architecture of sensor based agricultural information system for effective planning of farm activities. Proc. - 2004 IEEE Int. Conf. Serv. Comput. SCC 2004 93–100. ⟨https://doi.org/10.1109/SCC.2004.1357994⟩.

Chen, X., Zhang, F., Römheld, V., Horlacher, D., Schulz, R., Böning-Zilkens, M., Wang, P., Claupein, W., 2006. Synchronizing N supply from soil and fertilizer and N demand of winter wheat by an improved Nmin method. Nutr. Cycl. Agroecosystems 74, 91–98. https://doi.org/10.1007/s10705-005-1701-9.

Chen, Z., Miao, Y., Lu, J., Zhou, L., Li, Y., Zhang, H., Lou, W., Zhang, Z., Kusnierek, K., Liu, C., 2019. In-season diagnosis of winter wheat nitrogen status in smallholder farmer fields across a village using unmanned aerial vehicle-based remote sensing. Agronomy 9, 619. https://doi.org/10.3390/agronomy9100619.

Clivot, H., Mary, B., Valé, M., Cohan, J.P., Champolivier, L., Piraux, F., Laurent, F., Justes, E., 2017. Quantifying in situ and modeling net nitrogen mineralization from soil organic matter in arable cropping systems. Soil Biol. Biochem. 111, 44–59. https://doi.org/10.1016/j.soilbio.2017.03.010.

Crema, A., Boschetti, M., Nutini, F., Cillis, D., Casa, R., 2020. Influence of soil properties on maize and wheat nitrogen status assessment from Sentinel-2 data. Remote Sens. 12, 2175. https://doi.org/10.3390/rs12142175.

Davis, D.M., Gowda, P.H., Mulla, D.J., Randall, G.W., 2000. Modeling nitrate nitrogen leaching in response to nitrogen fertilizer rate and tile drain depth or spacing for Southern Minnesota, USA. J. Environ. Qual. 29, 1568–1581. https://doi.org/10.2134/jeq2000.00472425002900050026x.

Diacono, M., Rubino, P., Montemurro, F., 2013. Precision nitrogen management of wheat. a review. Agron. Sustain. Dev. 33, 219–241. https://doi.org/10.1007/s13593-012-0111-z.

Fraunhofer, 2020. "Sensorik zur schnellen elektronischen Detektion von Nitratkonzentrationen in Bodenproben" (Sensor technology for fast electronic detection of Nitrate concentrations in soil samples). 2020–03-03_Pressemitteilung_FraunhoferIISB_Nitratsensor-Future-IOT.pdf last accessed [11/02/2021 at 15:15].

Gnyp, M., Panitzki, M., Reusch, S., Bareth, G., 2016. Comparison between tractor-based and UAV-based spectrometer measurements in winter wheat. 13th Int. Conf. Precis. Agric. 1–10.

Grieder, C., Hund, A., Walter, A., 2015. Image based phenotyping during winter: a powerful tool to assess wheat genetic variation in growth response to temperature. Funct. Plant Biol. 42, 387–396. https://doi.org/10.1071/FP14226.

Hartmann, T.E., Yue, S., Schulz, R., Chen, X., Zhang, F., Müller, T., 2014. Nitrogen dynamics, apparent mineralization and balance calculations in a maize–wheat double cropping system of the North China Plain. Field Crops Res. 160, 22–30. https://doi.org/10.1016/j.fcr.2014.02.014.

Hategekimana, A., Schneider, D., Fossati, D., Mascher, F., 2012. Leistung und stickstoffeffizienz von Schweizer Weizensorten aus dem 20. Jhd. Agrar. Schweiz 3, 44–51.

Hausherr Lüder, R.M., Qin, R., Richner, W., Stamp, P., Streit, B., Herrera, J.M., Noulas, C., 2020. Small-scale variation in nitrogen use efficiency parameters in winter wheat as affected by N fertilization and tillage intensity. Sustain 12. https://doi.org/10.3390/su12093621.

Homolová, L., Malenovský, Z., Clevers, J.G.P.W., García-Santos, G., Schaepman, M.E., 2013. Review of optical-based remote sensing for plant trait mapping. Ecol. Complex. 15, 1–16. https://doi.org/10.1016/j.ecocom.2013.06.003.

Howard, P.J.A., 1965. The carbon-organic matter factor in various soil types. Oikos 15, 229–236.

Inselsbacher, E., Wanek, W., Strauss, J., Zechmeister-Boltenstern, S., Müller, C., 2013. A novel 15N tracer model reveals: plant nitrate uptake governs nitrogen transformation rates in agricultural soils. Soil Biol. Biochem. 57, 301–310. https://doi.org/10.1016/j.soilbio.2012.10.010.

Jarvis, S.C., Stockdale, E.A., Shepherd, M.A., Powlson, D.S., 1996. Nitrogen mineralization in temperate agricultural soils: processes and measurement. Adv. Agron. 57, 187–235. https://doi.org/10.1016/S0065-2113(08)60925-6.

Jin, Z., Prasad, R., Shriver, J., Zhuang, Q., 2017. Crop model- and satellite imagery-based recommendation tool for variable rate N fertilizer application for the US Corn system. Precis. Agric. 18, 779–800. https://doi.org/10.1007/s11119-016-9488-z.

Johnston, A.M., Bruulsema, T.W., 2014. 4R nutrient stewardship for improved nutrient use efficiency. Procedia Eng. 83, 365–370. https://doi.org/10.1016/j.proeng.2014.09.029.

Kabala, C., Karczewska, A., Gałka, B., Cuske, M., Sowiński, J., 2017. Seasonal dynamics of nitrate and ammonium ion concentrations in soil solutions collected using MacroRhizon suction cups. Environ. Monit. Assess. 189, 304. https://doi.org/10.1007/s10661-017-6022-3.

Kancheva, R., & Georgiev, G., 2013. Seasonal spectral response patterns of winter wheat canopy for crop performance monitoring. In *Remote Sensing for Agriculture,*

Ecosystems, and Hydrology XV (Vol. 8887, p. 88871V). International Society for Optics and Photonics. ⟨https://doi.org/10.1117/12.2029196⟩.

Kindred, D.R., Milne, A.E., Webster, R., Marchant, B.P., Sylvester-Bradley, R., 2015. Exploring the spatial variation in the fertilizer-nitrogen requirement of wheat within fields. J. Agric. Sci. 153 (1), 25–41. https://doi.org/10.1017/S0021859613000919.

Lassaletta, L., Billen, G., Grizzetti, B., Anglade, J., Garnier, J., 2014. 50 year trends in nitrogen use efficiency of world cropping systems: the relationship between yield and nitrogen input to cropland. Environ. Res. Lett. 9, 225–230. https://doi.org/10.1088/1748-9326/9/10/105011.

Lausch, A., Baade, J., Bannehr, L., Borg, E., Bumberger, J., Chabrilliat, S., Dietrich, P., Gerighausen, H., Glässer, C., Hacker, J.M., Haase, D., Jagdhuber, T., Jany, S., Jung, A., Karnieli, A., Kraemer, R., Makki, M., Mielke, C., Möller, M., Mollenhauer, H., Montzka, C., Pause, M., Rogass, C., Rozenstein, O., Schmullius, C., Schrodt, F., Schrön, M., Schulz, K., Schütze, C., Schweitzer, C., Selsam, P., Skidmore, A.K., Spengler, D., Thiel, C., Truckenbrodt, S.C., Vohland, M., Wagner, R., Weber, U., Werban, U., Wollschläger, U., Zacharias, S., Schaepman, M.E., 2019. Linking remote sensing and geodiversity and their traits relevant to biodiversity-Part I: soil characteristics. Remote Sens. 11, 2356. https://doi.org/10.3390/rs11202356.

Levy, L., Brabant, C., 2016. "Die Kunst, den Stickstoffdünger für einen - optimalen Ertrag und Proteingehalt von Weizen aufzuteilen" (The art of splitting nitrogen applications to optimise wheat yield and protein content). Agrar. Schweiz 7, 80–87.

Li, F., Mistele, B., Hu, Y., Chen, X., Schmidhalter, U., 2014. Reflectance estimation of canopy nitrogen content in winter wheat using optimised hyperspectral spectral indices and partial least squares regression. Eur. J. Agron. 52, 198–209. https://doi.org/10.1016/j.eja.2013.09.006.

Maltas, A., Charles, R., Pellet, D., Dupuis, B., Levy, L., Baux, A., Jeangros, B., Sinaj, S., 2015. "Evaluation de deux méthodes pour optimiser la fertilisation azotée des grandes cultures" (Evaluation of two methods to optimize nitrogen fertilization of field crops). Rech. Agron. Suisse 6, 84–93.

Manuilova, E. & Schuetzenmeister A., 2021. "mcr": Method Comparison Regression. R package version 1.2.2. ⟨https://CRAN.R-project.org/package=mcr⟩.

Meier, U., Bleiholder, H., Buhr, L., Feller, C., Hack, H., Heß, M., Lancashire, P.D., Schnock, U., Stauß, R., van den Boom, T., Weber, E., Zwerger, P., Peter Zwerger, C., 2009. "Das BBCH-System zur Codierung der phänologischen Entwicklungsstadien von Pflanzen" (The BBCH system to coding the phenological growth stages of plants-history and publications). Geschichte und Veröffentlichungen. J. Für Kult. 61, 41–52. https://doi.org/10.1113/jphysiol.2013.268730.

Murphy, D.V., Macdonald, A.J., Stockdale, E.A., Goulding, K.W.T., Fortune, S., Gaunt, J. L., Poulton, P.R., Wakefield, J.A., Webster, C.P., Wilmer, W.S., 2000. Soluble organic nitrogen in agricultural soils. Biol. Fertil. Soils 30, 374–387. https://doi.org/10.1007/s003740050018.

Norton, J., Ouyang, Y., 2019. Controls and adaptive management of nitrification in agricultural soils. Front. Microbiol. 10, 1–18. https://doi.org/10.3389/fmicb.2019.01931.

Ottow, J.C., 2011. "Mikrobiologie von Böden: Biodiversität, Ökophysiologie und Metagenomik", (Microbiology of soils: biodiversity, ecophysiology and metagenomics). Springe -J., Berl. Heidelb. https://doi.org/10.1007/978-3-642-00824-5.

Pan, L., Adamchuk, V.I., Martin, D.L., Schroeder, M.A., Ferguson, R.B., 2013. Analysis of soil water availability by integrating spatial and temporal sensor-based data. Precis. Agric. 14, 414–433. https://doi.org/10.1007/s11119-013-9305-x.

Pedersen, M.F., Gyldengren, J.G., Pedersen, S.M., Diamantopoulos, E., Gislum, R., Styczen, M.E., 2021. A simulation of variable rate nitrogen application in winter wheat with soil and sensor information-An economic feasibility study. Agric. Syst. 192, 103147 https://doi.org/10.1016/j.agsy.2021.103147.

Pinter Jr., P.J., Jackson, R.D., Elaine Ezra, C., Gausman, H.W., 1985. Sun-angle and canopy-architecture effects on the spectral reflectance of six wheat cultivars. Int. J. Remote Sens. 6 (12), 1813–1825. https://doi.org/10.1080/01431168508948330.

Preza Fontes, G., Bhattarai, R., Christianson, L.E., Pittelkow, C.M., 2019. Combining environmental monitoring and remote sensing technologies to evaluate cropping system nitrogen dynamics at the field-scale. Front. Sustain. Food Syst. 3, 1–13. https://doi.org/10.3389/fsufs.2019.00008.

Quan, Z., Huang, B., Lu, C., Shi, Y., Chen, X., Zhang, H., Fang, Y., 2016. The fate of fertilizer nitrogen in a high nitrate accumulated agricultural soil. Sci. Rep. 5, 1–9. https://doi.org/10.1038/srep21539.

R Core Team, 2020. R: A language and environment for statistical computing. R Foundation for Statistical Computing, Vienna, Austria. URL ⟨https://www.R-project.org/⟩ last accessed [11/02/2021 at 15:00].

Ravier, C., Jeuffroy, M.H., Gate, P., Cohan, J.P., Meynard, J.M., 2018. Combining user involvement with innovative design to develop a radical new method for managing N fertilization. Nutr. Cycl. Agroecosystems 110, 117–134. https://doi.org/10.1007/s10705-017-9891-5.

Rogovska, N., Laird, D.A., Chiou, C.P., Bond, L.J., 2019. Development of field mobile soil nitrate sensor technology to facilitate precision fertilizer management. Precis. Agric. 20, 40–55. https://doi.org/10.1007/s11119-018-9579-0.

Sainju, U.M., 2017. Determination of nitrogen balance in agroecosystems. MethodsX 4, 199–208. https://doi.org/10.1016/j.mex.2017.06.001.

Samborski, S.M., Tremblay, N., Fallon, E., 2009. Strategies to make use of plant sensors-based diagnostic information for nitrogen recommendations. Agron. J. 101, 800–816. https://doi.org/10.2134/agronj2008.0162Rx.

Scharf, P.C., Schmidt, J.P., Kitchen, N.R., Sudduth, K.A., Hong, S.Y., Lory, J.A., Davis, J. G., 2002. Remote sensing for nitrogen management. J. Soil Water Conserv 57, 518–524.

Sentek, 2011. Calibration Manual: for Sentek Soil Moisture. Stepney Sentek Pty Ltd 56.

Sieling, K., Kage, H., 2021. Apparent fertilizer N recovery and the relationship between grain yield and grain protein concentration of different winter wheat varieties in a

long-term field trial. Eur. J. Agron. 124, 126246 https://doi.org/10.1016/j.eja.2021.126246.

Signorell, A., 2021. "DescTools": Tools for Descriptive Statistics. R package version 0.99.42, ⟨https://cran.r-project.org/package=DescTools⟩.

Sinaj, S., Richner, W., 2017. Principles of fertilization of agricultural crops in Switzerland (PRIF 2017). Agrar. Schweiz 8 (6).

Spiess, E., Humphrys, C., Richner, W., Schneider, M.K., Piepho, H.P., Chervet, A., Prasuhn, V., 2020. Does no-tillage decrease nitrate leaching compared to ploughing under a long-term crop rotation in Switzerland? Soil Tillage Res. 199, 104590 https://doi.org/10.1016/j.still.2020.104590.

St. Luce, M., Whalen, J.K., Ziadi, N., Zebarth, B.J., 2011. Nitrogen dynamics and indices to predict soil nitrogen supply in humid temperate soils. Advances in Agronomy, 1st ed.,. Elsevier Inc. https://doi.org/10.1016/B978-0-12-385538-1.00002-0

Stevens, W.B., Hoeft, R.G., Mulvaney, R.L., 2005. Fate of nitrogen-15 in a long-term nitrogen rate study: II. Nitrogen uptake efficiency. Agron. J. 97, 1046–1053. https://doi.org/10.2134/agronj2003.0313.

Teralytic, 2020. ERALYTIC - WIRELESS NPK SOIL SENSOR. ⟨https://teralytic.com/⟩ last accessed [11/11/2021 at 15:10].

Terraquat, 2021. Applications of the Nitrate Online Measuring System (NITROM). TerrAquat GmbH - NITROM (Nitrat-Online-Messsystem) (terraquat-gmbh.com) last accessed [11/02/2021 at 15:10].

Tremblay, N., Bouroubi, M.Y., Vigneault, P., Bélec, C., 2011. Guidelines for in-season nitrogen application for maize (Zea mays L.) based on soil and terrain properties. F. Crop. Res. 122, 273–283. https://doi.org/10.1016/j.fcr.2011.04.008.

Walther, U., Menzi, H., Ryser, J.P., Flisch, R., Jeangros, B., Kessler, W., Maillard, A., Siegenthaler, A., Vuilloud, P.A., 1994. "Grundlagen für die Düngung im Acker-und Futterbau" (Principles of fertilization of agricultural crops in Switzerland, PRIF 1994). Agrar. Schweiz 1 (7), 1–40.

Wang, L., Zhou, X., Zhu, X., Guo, W., 2017. Estimation of leaf nitrogen concentration in wheat using the MK-SVR algorithm and satellite remote sensing data. Comput. Electron. Agric. 140, 327–337. https://doi.org/10.1016/j.compag.2017.05.023.

Yin, X., Beaudoin, N., Ferchaud, F., Mary, B., Strullu, L., Chlébowski, F., Clivot, H., Herre, C., Duval, J., Louarn, G., 2020. Long-term modelling of soil N mineralization and N fate using STICS in a 34-year crop rotation experiment. Geoderma 357, 113956. https://doi.org/10.1016/j.geoderma.2019.113956.

Yuzugullu, O., Lorenz, F., Fröhlich, P., Liebisch, F., 2020. Understanding fields by remote sensing: Soil zoning and property mapping. Remote Sens. 12, 1116. https://doi.org/10.3390/rs12071116.

Zaks, D.P.M., Kucharik, C.J., 2011. Data and monitoring needs for a more ecological agriculture. Environ. Res. Lett. 6, 014017 https://doi.org/10.1088/1748-9326/6/1/014017.